

# Marked enhancement of synthetic-antiferromagnetic coupling in subnanocrystalline FeCoB/Ru/FeCoB sputtered films

著者	齊藤 伸
journal or publication title	Applied Physics Letters
volume	89
number	3
page range	032511-1-032511-3
year	2006
URL	<a href="http://hdl.handle.net/10097/35008">http://hdl.handle.net/10097/35008</a>

doi: 10.1063/1.2234294

## Marked enhancement of synthetic-antiferromagnetic coupling in subnanocrystalline FeCoB/Ru/FeCoB sputtered films

Atsushi Hashimoto<sup>a)</sup> and Shin Saito

Department of Electronic Engineering, Tohoku University, Aoba-yama 6-6-05, Sendai 980-8579, Japan

Kazumi Omori, Hiroshi Takashima, and Tomonori Ueno

Hitachi Metals, Ltd., 2107-2 Yasugi-cho, Yasugi 692-8601, Japan

Migaku Takahashi

Department of Electronic Engineering, Tohoku University, Aoba-yama 6-6-05, Sendai 980-8579, Japan

and New Industry Creation Hatchery Center, Tohoku University, Aoba-yama 6-6-10, Sendai 980-8579, Japan

(Received 27 April 2006; accepted 30 May 2006; published online 21 July 2006)

Extremely large flopping field and saturation field were realized in an FeCoB/Ru/FeCoB sputtered film by using subnanocrystalline  $(\text{Fe}_{65}\text{Co}_{35})_{88}\text{B}_{12}$  soft magnetic material with high saturation magnetization. Phenomenological analysis of synthetic-antiferromagnetic coupling revealed that the bilinear coupling energy induced in this film was three times larger than that in a  $\text{Co}_{91}\text{Zr}_4\text{Nb}_5/\text{Ru}/\text{Co}_{91}\text{Zr}_4\text{Nb}_5$  film. This large bilinear coupling is thought to be the result of not only the suppression of ferromagnetic coupling due to the flat interface between the Ru and FeCoB layers but also the small Ru thickness for the first peak of 0.3 nm caused by the Fe-rich soft magnetic material. © 2006 American Institute of Physics. [DOI: 10.1063/1.2234294]

In a perpendicular recording medium, a thick soft magnetic underlayer (SUL) is indispensable for the magnetic flux closure in writing. The thick SUL is well known to induce degradation of surface roughness, occurrence of spike noise, and wide adjacent track erasure (WATE). To solve these problems, SULs with synthetic-antiferromagnetic (SAF) or synthetic-ferrimagnetic coupled structures have been widely investigated.<sup>1-5</sup> A SUL with SAF structure has the following two characteristics: (1) Néel walls are formed in the top and bottom soft magnetic (SM) layers in a pair<sup>6</sup> and (2) susceptibility along the film normal ( $\chi_{\perp}$ ) takes low value even if applying field angle is slightly tilted from the film normal. These properties are considered to be effective for the suppression of both spike noise and WATE.<sup>7</sup> High saturation magnetization ( $M_s$ ) materials retaining soft magnetic properties have also received much attention in connection with the mass fabrication of SULs. Thus, in order to improve the properties and manufacturability of the SUL mentioned above, it is essential to enhance the interlayer coupling induced in SULs with SAF structures using high- $M_s$  material such as FeCo alloys.

In this letter, we show that a large interlayer coupling can be induced in a SM/Ru/SM film by using a boron-added FeCo subnanocrystalline alloy with a high  $M_s$  of  $1520 \text{ emu/cm}^3$ .

Samples with the stacking structure of glass substrate/SM (30 nm)/Ru ( $d_{\text{Ru}}$  nm)/SM (30 nm) were fabricated by the dc magnetron sputtering method at room temperature under an Ar gas pressure of 0.6 Pa.  $(\text{Fe}_{65}\text{Co}_{35})_{88}\text{B}_{12}$  was selected as the SM layer material (hereafter simply FeCoB). For comparison,  $\text{Co}_{91}\text{Zr}_4\text{Nb}_5$  (hereafter simply CoZrNb;  $M_s$ :  $1090 \text{ emu/cm}^3$ ) which is well known to be a SUL material and  $(\text{Co}_{90}\text{Fe}_{10})_{80}\text{B}_{20}$  (hereafter simply CoFeB;  $M_s$ :  $1090 \text{ emu/cm}^3$ ) were also tested. Sputtering target of FeCoB was prepared by hot isostatic pressing of atomized

$\text{Fe}_{88}\text{B}_{12}$  and  $\text{Co}_{88}\text{B}_{12}$  powders.<sup>8</sup> The target-substrate distance and deposition rate were 30 mm and 2.01–2.60 nm/s for the SM layer and 110 mm and 0.15 nm/s for Ru layer, respectively. For the Ru layer, in particular, the deposition rate was strictly determined by the sputtering time versus film thickness plot evaluated by both a contact step height profiler and x-ray reflectivity. The composition of the sputtered FeCoB film was confirmed as Fe: 54.9, Co: 32.5, and B: 12.6 (at. %) by the inductively coupled plasma method; it was found that the target and film compositions were almost the same. The crystalline structure of the samples was exam-

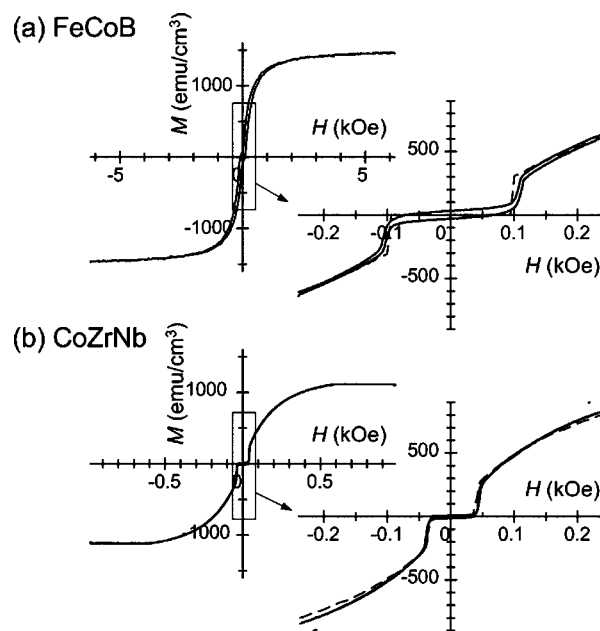


FIG. 1.  $M$ - $H$  loops for (a) FeCoB (30 nm)/Ru (0.3 nm)/FeCoB (30 nm) and (b) CoZrNb (30 nm)/Ru (0.6 nm)/CoZrNb (30 nm) samples. The figures on the left show a wide  $H$  range; the ones on the right are expansions around the flop field. Solid and dashed lines are experimental and calculated data, respectively.

<sup>a)</sup>Electronic mail: a-hash@ecei.tohoku.ac.jp

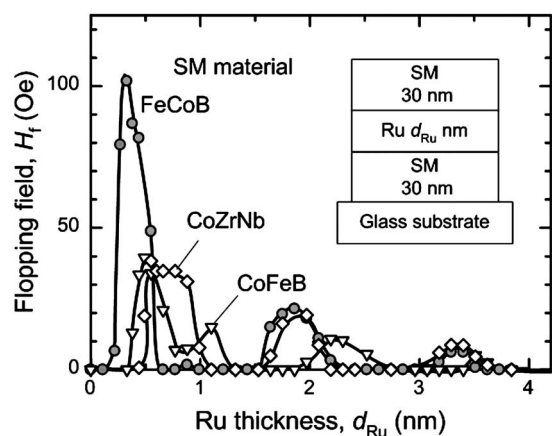


FIG. 2. Change in  $H_f$  as a function of  $d_{Ru}$  for (circle) FeCoB/Ru/FeCoB, (triangle) CoFeB/Ru/CoFeB, and (square) CoZrNb/Ru/CoZrNb stacked films. The thickness of all SM layers is fixed at 30 nm.

ined by x-ray diffraction (in-plane XRD) using Cu  $K\alpha$  radiation and transmission electron microscopy (TEM). In the case of XRD, since the incident angle of x rays was fixed to  $0.4^\circ$ , profiles reflected structural information from a depth of up to  $\sim 20$  nm from the film surface. The magnetic properties of the samples were evaluated by longitudinal Kerr equipment (LKE) and a vibrating sample magnetometer (VSM).<sup>9</sup>

Figure 1(a) show  $M$ - $H$  loops along the easy magnetization direction for an FeCoB (30 nm)/Ru (0.3 nm)/FeCoB (30 nm) film with strong interlayer coupling. For comparison,  $M$ - $H$  loops for a CoZrNb (30 nm)/Ru (0.6 nm)/CoZrNb (30 nm) film are shown in Fig. 1(b). As seen in Figs. 1(a) and 1(b), both samples show a small hysteresis in their  $M$ - $H$  loop, which suggests that the FeCoB and CoZrNb in these samples become soft magnetic. In the case of the magnetization process for a stacked film with interlayer coupling, magnetization is almost canceled out near zero field for both samples, which means the magnetic moments of the top and bottom SM layers assume an antiparallel alignment. As the external field increases, the magnetization flops at 41 Oe for (b) and 102 Oe for (a). Increasing the external field further brings the magnetic moments to saturation through a rotation-magnetized process.

Figure 2 shows the change in the flopping field,  $H_f$ , for FeCoB/Ru/FeCoB films as a function of  $d_{Ru}$ , as measured

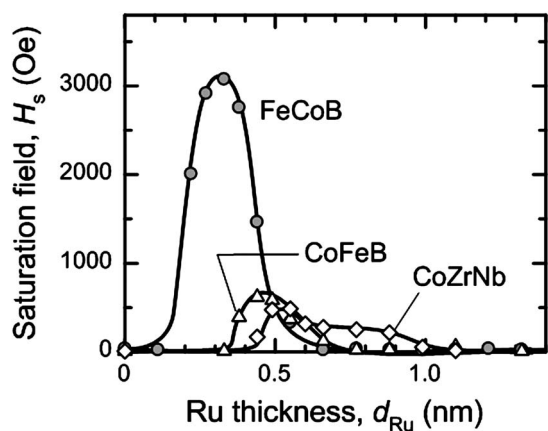


FIG. 3. Change in  $H_s$  as a function of  $d_{Ru}$  for (circle) FeCoB/Ru/FeCoB, (triangle) CoFeB/Ru/CoFeB, and (square) CoZrNb/Ru/CoZrNb stacked films. The thickness of all SM layers is fixed at 30 nm.

TABLE I.  $d_{Ru}$ ,  $M_s$ ,  $K_u$ ,  $J_1$ ,  $J_2$ , and  $\chi_\perp$  for SM/Ru/SM films. SM materials are FeCoB, CoFeB, and CoZrNb.

	$d_{Ru}$ (nm)	$M_s$ (emu/cm <sup>3</sup> )	$K_u$ (erg/cm <sup>3</sup> )	$J_1$ (erg/cm <sup>2</sup> )	$J_2$ (erg/cm <sup>2</sup> )	$\chi_\perp$
FeCoB	0.3	1520	$1.4 \times 10^4$	1.85	0.40	0.085
CoFeB	0.5	1090	$5.0 \times 10^3$	0.58	0.11	0.096
CoZrNb	0.6	1090	$4.6 \times 10^3$	0.55	0.13	0.095

by LKE. For comparison,  $H_f$  for stacked films using CoFeB or CoZrNb is also shown in the figure. In the case of the FeCoB/Ru/FeCoB film,  $H_f$  increases, attaining local maxima at  $d_{Ru}=3.3, 1.9, 0.9,$  and  $0.3$  nm. The largest  $H_f$  value is 102 Oe, observed at  $d_{Ru}=0.3$  nm. Although  $H_f$  also exhibits an oscillatory behavior in stacked films using CoFeB or CoZrNb, its maximum value is 40 Oe ( $d_{Ru}=0.5$  nm) or 38 Oe ( $d_{Ru}=0.6$  nm), respectively. Figure 3 shows the  $d_{Ru}$  dependence of the saturation field  $H_s$ , as measured by VSM. Here, the  $H_s$  values are determined at a magnetic field corresponding to 95% of  $M_s$ .  $H_s$  also shows an oscillatory behavior with  $d_{Ru}$ , and the magnitude of the maximum value of  $H_s$  for the FeCoB/Ru/FeCoB film is larger than those for stacked films using CoFeB or CoZrNb. These enhancements of  $H_f$  and  $H_s$  for the FeCoB/Ru/FeCoB film clearly indicate that a large interlayer coupling is induced between SM layers.

Table I tabulates the saturation magnetization  $M_s$ , uniaxial magnetic anisotropy energy  $K_u$ , coefficients of bilinear and biquadratic coupling energy,  $J_1$  and  $J_2$ , and susceptibility along the film normal,  $\chi_\perp$ , for SM/Ru/SM films with the maximum  $H_f$  value for each SM material. Here,  $M_s$ ,  $K_u$ , and  $\chi_\perp$  represent experimental data. The values of  $J_1$  and  $J_2$  were determined by fitting calculated  $M$ - $H$  loops to  $M$ - $H$  experimental loops.<sup>5,9</sup> (See typical results of fitted  $M$ - $H$  loops in Fig. 1.) The magnitude of  $J_1$  for the FeCoB/Ru/FeCoB film is 1.85 erg/cm<sup>2</sup>, which is three times larger than that for CoZrNb ( $J_1$ :0.55 erg/cm<sup>2</sup>). The FeCoB/Ru/FeCoB film shows the lowest  $\chi_\perp$  among the samples studied. Thus, FeCoB/Ru/FeCoB is regarded as a promising candidate for SUL in terms of having high  $M_s$  and strong synthetic-antiferromagnetic coupling.

Figure 4 shows in-plane XRD profiles for SM/Ru/SM films using FeCoB, CoFeB, and CoZrNb as SM layer materials. Although a broad diffraction band can be observed at around  $44^\circ$  for all samples, no distinct diffraction peaks due

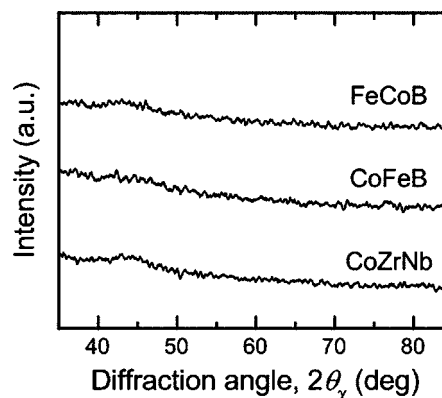


FIG. 4. In-plane XRD profiles for SM/Ru/SM films. SM materials are FeCoB, CoFeB, and CoZrNb.

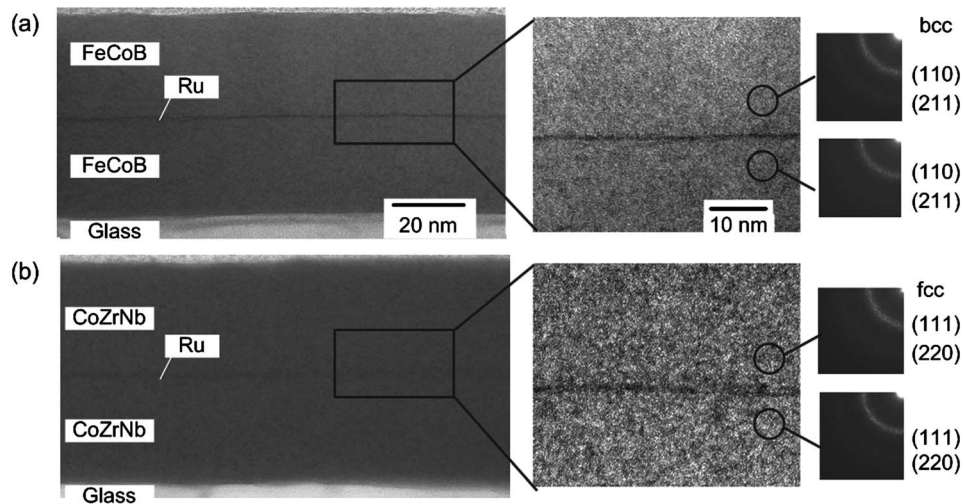


FIG. 5. Cross-sectional TEM images for (a) FeCoB (30 nm)/Ru (0.3 nm)/FeCoB (30 nm) and (b) CoZrNb (30 nm)/Ru (0.3 nm)/CoZrNb (30 nm) films. The figures on the right show electron diffraction images of the FeCoB or CoZrNb layer obtained by using a 5 nm spot probe.

to a crystalline phase are detected. Figures 5(a) and 5(b) show bright field images of whole samples and cross-sectional TEM images of an enlarged region near the Ru layer for FeCoB (30 nm)/Ru (0.3 nm)/FeCoB (30 nm) and CoZrNb (30 nm)/Ru (0.3 nm)/CoZrNb (30 nm) films, respectively. Also shown for each sample are electron diffraction patterns for the top and bottom SM layers obtained by a 5 nm spot probe. In the bright field images, SM layers have homogeneous gray contrast in all samples. The film surface and the SM/Ru interface are quite smooth; only small undulations with a long period can be observed, corresponding to the surface roughness of the glass substrate. In the electron diffraction images, a broadened first ring and indistinct second ring patterns can be observed; in terms of crystalline phase, these diffraction rings are identified as (110) and (211) planes of the bcc structure for the FeCoB layer and (111) and (200) planes of the fcc structure for the CoZrNb layer, respectively. These results indicate that the present SM layers consist of extremely small grains whose crystal axes are oriented randomly in three-dimensional space. Thus, FeCoB and CoZrNb have a subnanocrystalline microstructure according to the probe diameter and ringlike electron diffraction.

On the basis of the above results, the causes of the large bilinear coupling induced in the FeCoB/Ru/FeCoB film are thought to be the following: (1) suppression of the ferromagnetic coupling (Néel coupling) due to interfacial smoothness and (2) shift to the first peak caused by the Rundeman-Kittel-Kasuya-Yoshida-like interlayer coupling<sup>10</sup> on small Ru thick-

ness. Especially in the latter factor, the concentration ratio of Fe to Co, is thought to affect oscillatory behavior. The dependence of interlayer coupling on compositional ratio in FeCo alloys retaining subnanocrystalline structure will be reported in a future publication.<sup>11</sup>

The authors thank Goto from Ohara Inc. for contributing the substrates used in this experiment.

<sup>1</sup>S. Saito, K. Hirai, A. Hashimoto, M. Tsunoda, and M. Takahashi, *J. Magn. Soc. Jpn.* **27**, 224 (2003).

<sup>2</sup>S. C. Byeon, A. Misra, and W. D. Doyle, *IEEE Trans. Magn.* **40**, 2386 (2004).

<sup>3</sup>B. R. Acharya, J. N. Zhou, M. Zheng, G. Choe, E. N. Abarra, and K. E. Johnson, *IEEE Trans. Magn.* **40**, 2383 (2004).

<sup>4</sup>K. Tanahashi, R. Arai, and Y. Hosoe, *IEEE Trans. Magn.* **41**, 577 (2005).

<sup>5</sup>M. Desai, A. Misra, and W. D. Doyle, *IEEE Trans. Magn.* **41**, 3151 (2005).

<sup>6</sup>S. Iida, S. Iwasaki, Y. Iwama, H. Kobayashi, Y. Sakurai, T. Nagashima, and S. Watanabe, *Engineering of Magnetic Thin Films* (Maruzen, Tokyo, 1977), p. 231, in Japanese.

<sup>7</sup>A. Hashimoto, S. Saito, and M. Takahashi, *J. Appl. Phys.* **99**, 08Q907 (2006).

<sup>8</sup>H. Ueno, T. Ueno, and S. Yokoyama, Digest of the 28th Annual Conference of Magnetics in Japan, Okinawa, Japan, 21–24 September 2004 (unpublished), Paper No. 21pB-4.

<sup>9</sup>J. F. Bobo, H. Kikuchi, O. Redon, E. Snoeck, M. Piecuch, and R. L. White, *Phys. Rev. B* **60**, 4131 (1999).

<sup>10</sup>S. S. P. Parkin, *Phys. Rev. Lett.* **67**, 3598 (1991).

<sup>11</sup>A. Hashimoto, S. Saito, D. Y. Kim, H. Takashima, T. Ueno and M. Takahashi, Proceedings of the IEEE International Magnetic Conference, San Diego, 8–12 May 2006.